Proceedings of the 9th World Congress on Mechanical, Chemical, and Material Engineering (MCM'23)
Brunel University, London, United Kingdom - August 06-08, 2023
Paper No. ICMIE 107
DOI: 10.11159/icmie23.107

The Importance of the Cavitation Effective Yield Stress and the Hole Slenderness Ratio for Accurate Predictions of Ballistic Limit Velocities

Rami Masri
Department of Mechanical Engineering, Braude College of Engineering, Karmiel, Israel
E-mail: ramim@braude.ac.il

Abstract – Perforation and penetration mechanics research is mostly governed by experimental and numerical investigations while analytical models are less available due to the extremely complicated nature of the subject. Sufficiently thick ductile targets are perforated by rigid, nose-pointed projectiles in a ballistic process whose dominant failure mode is ductile hole enlargement. Several recent studies have shown that for perforation process by ductile hole formation, the specific cavitation energy, which reflects the target material resistance to steady hole expansion, is essential for analytical predictions of ballistic limit velocities. The ballistic limit velocity is the minimum impact speed that is required for complete perforation of a given target by a given projectile. A logarithmic formulation for the specific cavitation energy of metal targets, which is based on the concepts of (spherical cavitation) effective yield stress and hole slenderness ratio, is shown in several recent studies to be very useful for analytical predictions of ballistic limit velocities. The logarithmic formulation for the specific cavitation energy is presented, and the concepts of cavitation effective yield stress and hole slenderness ratio are reviewed and discussed regarding their importance for accurate analytical predictions of ballistic limit velocities. The present article is a review of these two concepts and their usefulness in perforation mechanics.

***Keywords*:** Perforation mechanics; Ballistic limit velocity; Ductile hole formation; Specific cavitation energy; Cavitation effective yield stress; Hole slenderness ratio

1. Introduction

The resistance of a target material to penetration is the most critical parameter when designing protective systems. The dominant failure mode of a protective system depends on the characteristics of projectile and shielding and on the impact conditions. Perforation and penetration mechanics research is governed by experimental and numerical studies while analytical models are less available due to the extremely complicated nature of the subject [1]. The present paper is focused on a review of an analytical model for perforation by ductile hole growth process, in which a near-rigid, pointed-nose projectile is impacting a softer ductile target. The ballistic limit velocity V_b is the projectile minimum impact speed that is required for complete perforation of the target (without a residual velocity upon exiting the target). In the present paper a recent ballistic model, which was shown to be very useful for analytical predictions of ballistic limit velocities, is reviewed.

Analytical methods for ductile hole enlargement date back to the pioneering studies by Bishop, Hill and Mott [2] and Hill [3], where spherical and cylindrical cavity expansion models were used for estimation of the material hardness. Later, plane-strain, cylindrical cavity expansion models [4-11] have been shown to provide accurate ballistic limit predictions only for perforation of ductile targets under plane-strain conditions. However, such plane-strain models are not accurate enough for ballistic limit predictions in other stress-state conditions. The cavity expansion analysis under plane-stress conditions [12] has shown that the specific expansion energy, supplied by the internal pressure for creating a new hole volume unit, approaches an asymptotic value. This energy saturation level, which is identified (in section 5 of [12]) with cavitation pressures for plane-strain and spherical deformation patterns, reflects the resistance of the material target to steady hole expansion, and is denoted in [12] as the specific cavitation energy s_c.

During a perforation process, recoverable elastic energy and dissipated plastic energy consume the work done by the projectile for creating the penetration tunnel. For near-rigid, nose-pointed projectiles that penetrate softer ductile targets, this elastoplastic work can be approximated with the aid of the specific cavitation energy s_c, and the ballistic limit velocity V_b can be predicted by a simple energy balance (see section 2). The hole slenderness ratio (the ratio between plate thickness h and projectile shank diameter D, namely h/D) is observed in [13] to affect the specific cavitation energy and the ballistic limit velocity. The heuristic approach in [14] has inspired a logarithmic expression for s_c of monolithic metal targets, which considers the hole slenderness ratio effect. In this logarithmic formulation the spherical cavitation effective yield stress (Y_c^S) is shown to play an essential role. Comprehensive comparisons to experimental data in [14-16] have shown that the logarithmic formulation of s_c leads to accurate predictions of ballistic limit velocities, and in [17] it is observed that the accuracy of the analytical predictions is at least comparable to the accuracy of numerical simulation results. In the study [18], four ductile hole enlargement models have been compared for their ability to predict ballistic limits of aluminium plates impacted by 7.62 mm armour piercing bullets (APM2 bullets) at normal incidence. A very large database of ballistic limit tests (more than 1600 experimental results for 24 different aluminium alloys) is used to evaluate the accuracy of these four models. The best performing model is found to be the logarithmic formulation for s_c suggested in [14], which depends on the effective yield stress Y_c^S and considers the hole slenderness ratio h/D.

While the logarithmic formulation of s_c is valid for an arbitrary stress-strain relation, due to the general definition of the (spherical cavitation) effective yield stress Y_c^S, which is based on the classical Lambert function [19], further approximate expressions of Y_c^S are given in [17] for several strain-hardening laws, in terms of classical functions from mathematical physics (Riemann Zeta, Euler Gamma, polylogarithm and Gauss hypergeometric functions).The logarithmic formulation of s_c is presented in section 2.1, the concept of the effective yield stress is discussed in section 3 and the hole slenderness ratio effect is discussed in section 4.

2. Analytical Prediction of Ballistic Limit Velocity

Ballistic limit velocity of a (thick enough) ductile protective plate of thickness h, perforated at normal incidence by a near-rigid, nose-pointed projectile of mass M and shank diameter D (Fig. 1), can be estimated by an energy-balance. The elastoplastic work, consumed in expanding the perforation tunnel, can be approximated by

$$W = \left(\frac{\pi D^2}{4}\mathrm{h}\right) s_c \tag{1}$$

where the specific cavitation energy s_c reflects the target material resistance to quasi-static expansion of the perforation hole. The ballistic limit velocity V_b of a ductile monolithic plate is obtained by equating the work done by the projectile in expanding the perforation tunnel, Eq. (1), with the projectile ballistic limit kinetic energy $\frac{1}{2}MV_b^2$ (after [12])

$$V_b = \sqrt{2R_t/\gamma_p} \qquad R_t = hs_c \qquad \gamma_p = \frac{4M}{\pi D^2} \tag{2}$$

Parameter γ_p is the projectile areal density, which reflects the projectile perforation potential, and R_t is the (combined) target perforation resistance, of target material and thickness, to quasi-static cavitation of the perforation tunnel.

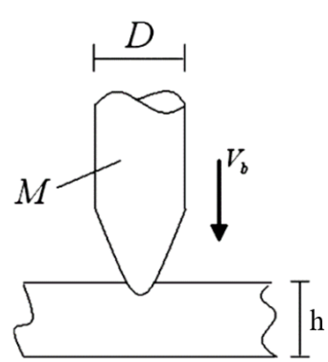

Fig. 1: Plate of thickness h is perforated by a nose-pointed projectile of mass M and shank diameter D (figure is taken from [12]).

2.1. Logarithmic Formulation of the Specific Cavitation Energy s_c

The specific cavitation energy concept has been used in [14] to demonstrate the ballistic equivalence of several aluminium alloys (similar ballistic limits for the same threats), and this observation has inspired a heuristic approach in [14] [14] that leads to the following logarithmic formulation of s_c for monolithic ductile targets

$$s_c = \frac{Y_c^S}{\sqrt{3}}\left[1 + \ln\left(\frac{h}{3D}\frac{E}{\sqrt{3}Y_c^S}\right)\right] \tag{3}$$

where E is the target elastic modulus. This formulation suggests a logarithmic effect of the hole slenderness ratio h/D and reflects the essential role of the effective yield stress Y_c^S for ballistic limit predictions by formula (2). Due to this formulation of s_c, different alloys of the same metal (namely alloys with practically the same elastic properties) are ballistically equivalent (namely have practically the same ballistic limits) if their effective yield stresses are close enough (see section 3). More general definition of two different targets (different materials and thicknesses) which are ballistically equivalent for the same threat are targets who have practically the same perforation resistance, namely

$$R_{t1} = R_{t1} \Rightarrow h_1 s_{c1} = h_2 s_{c2} \tag{4}$$

This definition for ballistically equivalent targets was validated by finite element simulations for aluminium and steel targets in [20] and is discussed in the next section. Here it should be mentioned that the cavitation pressure needed for steady cylindrical cavity expansion under plane-strain conditions [4-11, 21] is shown in [15], [17] and [20] to be suitable only for ballistic limit predictions under perforation conditions that are close to plane-strain ($h/D \approx 3$). However, the logarithmic formulation (3) is shown, by comprehensive comparisons to experimental data [14-18], to be accurate enough for ballistic limit predictions of many target/threat combinations and over a wide range of h/D ratios.

3. The Spherical Cavitation Effective Yield Stress Y_c^S

The exact definition of the (spherical cavitation) effective yield stress Y_c^S was first given in [22]. The motivation in [22] was to suggest a well-defined way for approximating an arbitrary stress–strain response with an effective elastic/perfectly-plastic behaviour, to simplify the analysis of dynamic spherical cavitation in metals. The definition of Y_c^S is based on equating the quasi-static spherical cavitation pressure for compressible Mises (Tresca) solid, which is characterized by an arbitrary stress–strain response, (the following expression is derived in [23] and reformulated in [14])

$$p_c^S = \int_0^\infty \frac{\sigma(\bar{\varepsilon})d\bar{\varepsilon}}{\exp\left(\frac{3}{2}\bar{\varepsilon} - S\right) - 1 + S} \qquad S = 2\beta\frac{\sigma(\bar{\varepsilon})}{E} \tag{5}$$

with its exact version for elastic/perfectly-plastic behaviour, where the constant yield stress Y is replaced by the effective yield stress Y_c^S. Here $\beta = 1 - 2\nu$ is an elastic compressibility measure, with ν for Poisson ratio, and $\bar{\varepsilon} = \varepsilon + \beta\frac{\sigma(\varepsilon)}{E}$ with ε for the effective elastoplastic (total) strain and $\sigma = \sigma(\varepsilon)$ is an arbitrary target material stress-strain curve. Hence, it is straightforward to calculate the function $\sigma(\bar{\varepsilon})$ in the integrand of Eq. (5), and p_c^S can be obtained for arbitrary stress–strain curves by simple numerical integration procedure. While the exact definition leads to a cumbersome implicit equation for Y_c^S, a much compact form of this equation under the practical assumption $\frac{Y_c^S}{E} \ll 1$ is (after [22])

$$\frac{2Y_c^S}{3}\left\{1 + \ln\left[\frac{2E}{3(1+\beta)Y_c^S}\right]\right\} = p_c^S \tag{6}$$

The following closed-form expression for the physical solution of Y_c^S is recently derived in [19]

$$Y_c^S = -\frac{3p_c^S}{2W_{-1}(x)} \qquad x = -\frac{9(1+\beta)p_c^S}{4eE} \tag{7}$$

where $W_{-1}(x)$ is the non-principal branch of the Lambert function. The Lambert function is a classical function from mathematical physics with many applications, and the use of this function here eliminates the need for solving the physical value of Y_c^S from Eq. (6) by numerical procedure. Further useful approximations of Y_c^S are given in [17] for common strain-hardening laws in terms of different classical functions from mathematical physics (Riemann Zeta, Euler Gamma, Polylogarithm and Gauss hypergeometric functions). As an example, for the modified Ludwik power-hardening law $\sigma = Y\left(\frac{\varepsilon}{\varepsilon_y}\right)^n$ (for $\varepsilon \geq \varepsilon_y$), where $\varepsilon_y = Y/E$ is the target yield strain and n is the hardening exponent, a tight lower bound for the exact value of Y_c^S is obtained by

$$Y_c^S = \left[1 + \frac{\phi^n F(n) - \frac{1}{n} - \ln(\phi)}{\ln\left(\frac{\phi}{1+\beta}\right)}\right] Y \qquad \phi = \frac{2}{3\varepsilon_y} \qquad F(n) = \zeta(1+n)\Gamma(1+n) \tag{8}$$

where ζ and Γ are the well-known Riemann Zeta and Euler Gamma functions, and $F(n) \simeq 1/n + 0.73n$ for common metals [15]. The definition of Y_c^S suggests an effective elastic/perfectly-plastic response with the same quasi-static spherical cavitation pressure p_c^S (and the same elastic properties E and ν) as of the actual metal with the true stress–strain curve. In [14] it is shown that Y_c^S lumps different strain-hardening responses of five aluminium alloys into similar effective yield stresses of about 337 MPa (Fig. 2), and those alloys were shown in [14], by experimental data, to be ballistically equivalent.

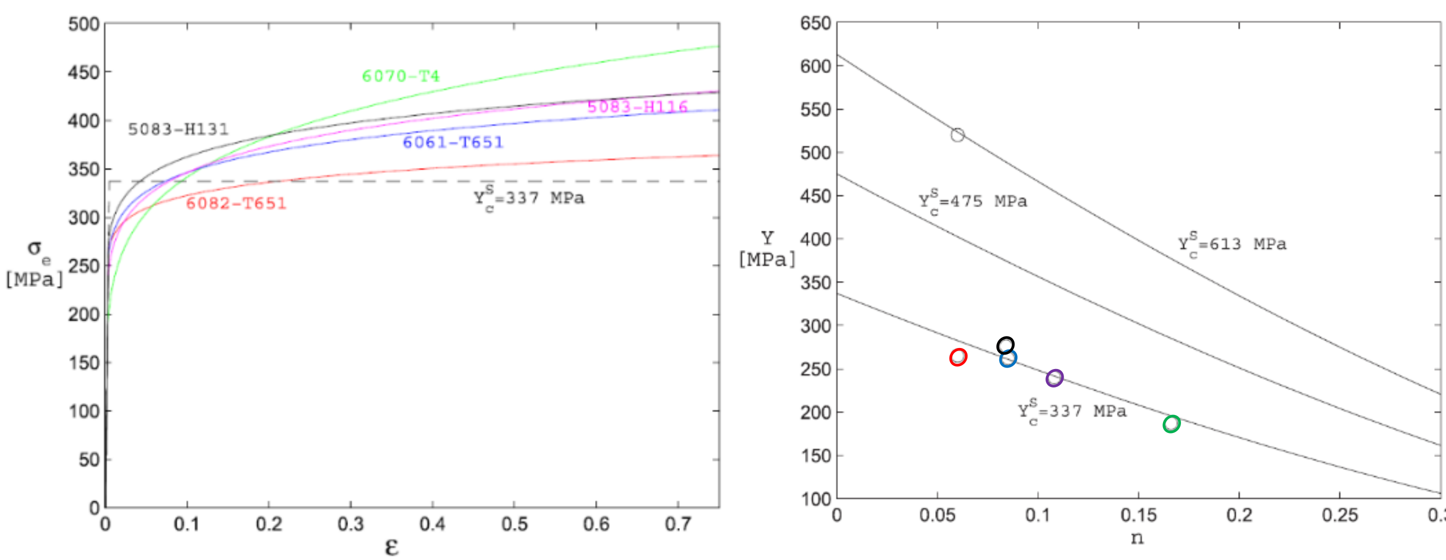

Fig. 2: **Left** - Stress-strain curves of five ballistically equivalent aluminium alloys. The dashed line represents the effective elastic/perfectly-plastic response with an effective yield stress of 337 MPa. **Right** - Three Y_c^S curves in an (n, Y) coordinate system, due to formula (8), for different aluminium alloys with $E = 70\ GPa$ and $\nu = 1/3$. The points (n, Y) of the five ballistically equivalent aluminium alloys in the left figure are shown to be near the $Y_c^S = 337\ MPa$ curve (Both figures are taken from [14]).

Comprehensive finite element simulations study is performed in [20] for validating the general definition of two ballistically equivalent targets (4) by using abrasion resistant steel targets (Hardox 400), high-strength aluminium alloy targets (AA6061-T651) and annealed aluminium alloy targets (AA6070-O) that are perforated by projectiles which simulate the steel core of a 7.62 mm APM2 bullet. In Fig. 3 the model which is based on the logarithmic formulation (3) leads to practically ballistic equivalence between the steel and the aluminium targets, while the general formula for the Mises plane-strain cylindrical cavitation presssure (derived in [21] and reformulated in [14])

$$p_c^M = \int_0^\infty \frac{\sigma(\bar{\varepsilon})d\bar{\varepsilon}}{\exp\left(\sqrt{3}\bar{\varepsilon} - S\right) - 1 + S} \qquad \bar{\varepsilon} = \varepsilon + 0.65\beta\frac{\sigma(\varepsilon)}{E} \qquad S = 1.7\beta\frac{\sigma(\bar{\varepsilon})}{E} \tag{9}$$

is not good enough for accurate analytical predictions of ballistic limit velocities.

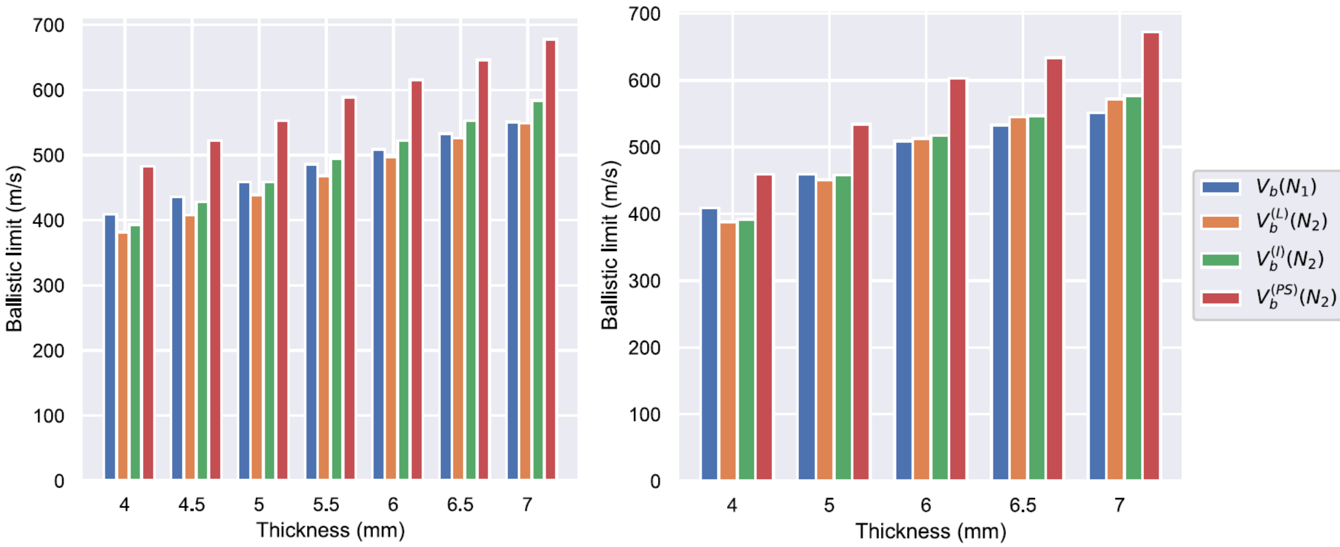

Fig. 3: Comparing numerical simulation predictions $V_b(N_1)$ of ballistic limits for 4.0 to 7.0 mm Hardox 400 plates with numerical ballistic limit predictions for ballistically-equivalent AA6070-O plates (on the **left**) and AA6061-T651 plates (on the **right**), determined by using the logarithmic (L) (Eq. (3)), integral (I), and plane-strain (PS) (Eq. (9)) variants for s_c (Both figures are taken from [20]). The integral formulation of s_c has not discussed in the present paper (for details on this formulation refer to [15-17]).

In [19] it is suggested that for common metals, the value of the 'material' parameter x in formula (7) is likely to be in the range $-5 \cdot 10^{-2} < x < -0.4 \cdot 10^{-2}$. Here it is added that by suggesting the approximation $W_{-1}(x) \simeq a + b ln(-x)$ and determining the constants a and b by the requirement that this approximation will be exact at the lower and the upper boundaries $x = -5 \cdot 10^{-2}$ and $x = -0.4 \cdot 10^{-2}$, the approximation obtained is $W_{-1}(x) \simeq -0.8915 + 1.2045\ln(-x)$. Substitution of this approximation in (7) leads to an excellent tight upper bound for Y_c^S

$$Y_c^S = \frac{p_c^S}{0.746 + 0.803\ln\left[\frac{E}{(1+\beta)p_c^S}\right]} \tag{10}$$

For arbitrary stress–strain curves the exact value of p_c^S is calculated by numerical integration of (5), while approximate formulae of p_c^S for linear, modified Ludwik and combined Ludwik-Voce stress–strain curves are given in the appendices of [15] and [17]. As an example, excellent approximation of p_c^S (Eq. (5)) for the modified Ludwik hardening law is (after [15])

$$p_c^S = \frac{2}{3} Y \left[1 + \phi^n \mathrm{F(n)} - \frac{1}{n} - \ln(1+\beta) \right] \tag{11}$$

This expression is more accurate than the integral formula used in [24] for incompressible media since expression (11) considers the effect of the material (elastic) compressibility β. By using Eq. (11) for the value of p_c^S in expression (10), the approximate value of Y_c^S is found to be slightly better than the one obtained from formula (8).

4. The effect of the hole slenderness ratio h/D

A comprehensive comparison with experimental data in [15] has demonstrated that the ratio between the ballistic limits of two targets, from the same metal but with thicknesses kh and h $(k > 1)$, against the same threat, is higher than the commonly accepted value of $\sqrt{k}$. While the ratio of $\sqrt{k}$ is due to the plane-strain cylindrical cavitation pressure [4-11], by using the logarithmic formulation (3), the following expression has been found in [15] to be more accurate than $\sqrt{k}$

$$\frac{V_b(kh)}{V_b(h)} = \sqrt{k} \sqrt{1 + \frac{\ln(k)}{1 + \ln\left(\frac{h}{3D}\frac{E}{\sqrt{3}Y_c^S}\right)}} \tag{12}$$

This expression reflects the logarithmic effect of the hole slenderness ratio h/D, which is not included in ballistic perforation models that are based on the plane-strain cylindrical cavitation pressure [4-11], and in [15] it is shown that expression (12) agrees very well with the experimental data (see Table 1 in [15]). The logarithmic effect of the h/D ratio is supported in [18] by a very large database of ballistic limit tests (more than 1600 experimental results for 24 different aluminium alloys perforated by 7.62 mm APM2 bullets) and is supported by comprehensives finite element simulations in [20] and in [25-26]. While the logarithmic formulation of s_c in Fig. 4 leads to accurate predictions of V_b, the plane-strain cylindrical cavitation pressure is clearly not a good enough model for s_c.

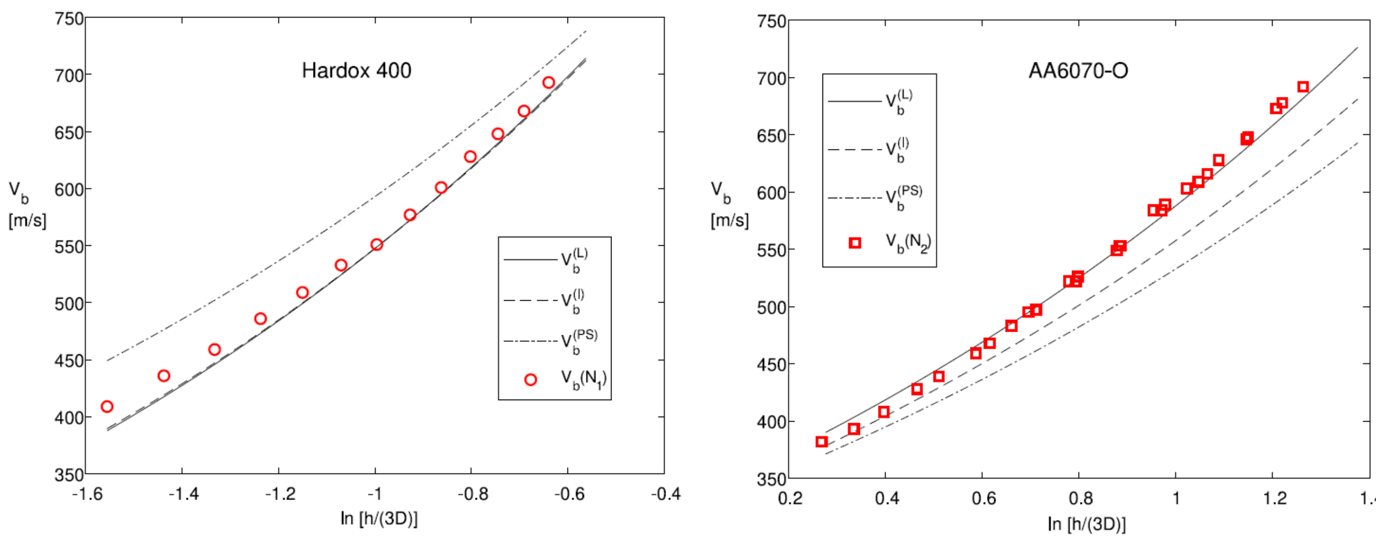

Fig. 4: Comparison of numerical ballistic limit data $V_b(N_1)$ for Hardox 400 targets (circle markers) and $V_b(N_2)$ for AA6070-O plates (square markers) with ballistic limit predictions due to the logarithmic (L) (Eq. (3)), integral (I), and plane-strain (PS) (Eq. (9)) variants for s_c (Both figures are taken from [20]). The integral formulation of s_c has not discussed in the present paper (for details on this formulation refer to [15-17]).

5. Conclusion

The specific cavitation energy is an essential parameter needed for analytical predictions of ballistic limit velocities in ductile perforation process (ductile targets that are impacted by near-rigid, nose-pointed projectiles). The plane-strain cylindrical cavitation pressure is clearly not a good enough model for the specific cavitation energy, and it is limited only to ductile perforations under plane-strain conditions ($h/D \approx 3$).

The logarithmic formulation of the specific cavitation energy (Eq. (3)) is found to be accurate enough for ballistic limit predictions of many target/threat combinations and over a wide range of h/D ratios. This logarithmic formulation depends on the concepts of (spherical cavitation) effective yield stress Y_c^S and hole slenderness ratio h/D. The effective yield stress Y_c^S lumps the actual stress-strain response of an arbitrary metal into a single, useful effective yield stress for ballistic limit predictions. The hole slenderness ratio h/D has a logarithmic effect on the specific cavitation energy. Hence, the ratio between the ballistic limits of two targets, from the same metal but with thicknesses kh and h against the same threat, is higher than the commonly accepted value of $\sqrt{k}$, and a more accurate ratio is given in expression (12).

Acknowledgements

R. Masri would like to express his gratitude to D. Durban, S. Ryan and T. Cohen which were collaborators for several studies presented in this paper.

References

[1] C. E. Anderson, "Analytical models for penetration mechanics: A review," *Int. J. Impact Eng.,* vol. 108, pp. 3-26, 2017.
[2] R. F. Bishop, R. Hill, and N. F. Mott, "The theory of indentation and hardness". *Proc. Math. Phys. Soc.,* vol 57, pp. 147-159, 1945.
[3] R. Hill, *The mathematical theory of plasticity*. Oxford University Press, 1950.
[4] M. J. Forrestal and T. L. Warren, "Perforation equations for conical and ogival nose rigid projectiles into aluminium target plates," *Int. J. Impact Eng.,* vol. 36, pp. 220-225, 2009.
[5] J. Johnsen, J. K. Holmen, T. L. Warren and T. Børvik, "Cylindrical cavity expansion approximations using different constitutive models for the target material," *Int. J. Protect Struct.*, vol. 9, pp. 199-225, 2018.
[6] M. J. Forrestal, B. Lim and W. Chen, "A scaling law for APM2 bullets and aluminum armor plates," *Exp. Mech.,* vol. 59, pp. 121-123, 2019.
[7] M. J. Forrestal, T. L. Warren and J. K. Holmen, "Ballistic-limit velocities for 7.62 mm APM2 bullets and aluminum alloy armor plates," *J. Dyn. Behav. Mater.,* vol. 7, pp. 624-627, 2021.
[8] M. J. Forrestal, T. L. Warren, "Perforation of Steel Plates with 7.62 mm APM2 Bullets," *J. Dyn. Behav. Mater.,* vol. 8, pp. 418-421, 2022.
[9] G. Ben-Dor, A. Dubinsky and T. Elperin, *High-speed penetration dynamics: engineering models and methods*. World Scientific, 2013.
[10] J. D. Walker, *Modern impact and penetration mechanics*. Cambridge University Press, 2021.
[11] R. Dubey, R. Jayaganthan, D. Ruan, N. K. Gupta, N. Jones and R. Velmurugan, "Ballistic perforation and penetration of 6xxx-series aluminium alloys: A review," *Int. J. Impact Eng.,* vol. 172, 104426, 2023.
[12] R. Masri, T. Cohen and D. Durban, "Enlargement of a circular hole in a thin plastic sheet: Taylor-Bethe controversy in retrospect," *Q. J. Mech. Appl. Math.,* vol. 63, pp. 589-616, 2010.
[13] T. Cohen, R. Masri and D. Durban, "Ballistic limit predictions with quasi-static cavitation fields," *Int. J. Protect Struct.,* vol. 1, pp. 235-255, 2010.
[14] R. Masri, "Ballistically equivalent aluminium targets and the effect of hole slenderness ratio on ductile plate perforation," *Int. J. Impact Eng.,* vol. 80, pp. 45-55, 2015.
[15] R. Masri and D. Durban, "Ballistic limit predictions for perforation of aluminium armour plates by rigid nose-pointed projectiles," *Int. J. Impact Eng.,* vol. 131, pp. 291-303, 2019.
[16] R. Masri and D. Durban, "Comparison of experimental and numerical simulation data for ballistic velocities of aluminium plates with predictions of available analytical formulae," *Int. J. Impact Eng.,* vol. 141, 103563, 2020.

[17] R. Masri, "Practical formulae for predicting the ballistic limit velocity of armour perforation by ductile hole growth," *Int. J. Impact Eng.,* vol. 167, 104219, 2022.
[18] R. Shannon, H. N. Long, G. Denver and S. J. Cimpoeru, "The scaling law for predicting the ballistic performance of aluminium alloy targets perforated in ductile hole," *Int. J. Impact Eng.,* vol. 116, pp. 34-50, 2018.
[19] R. Masri, "Exact formula for the effective yield stress of metals with arbitrary stress–strain curves," *Int. J. Impact Eng.,* vol. 177, 104589, 2023.
[20] R. Masri R and S. Ryan, "Ballistic limit predictions of non-identical layered targets perforated in ductile hole formation," *Int. J. Impact Eng.,* vol. 171, 104391, 2023.
[21] R. Masri R and D. Durban D, "Cylindrical cavity expansion in compressible Mises and Tresca solids," *Eur. J. Mech. A Solids*, vol. 26, pp. 712-727, 2007.
[22] R. Masri R and D. Durban, "Dynamic spherical cavity expansion in an elastoplastic compressible Mises solid," *J. Appl. Mech.,* vol. 72, pp. 887-898, 2005.
[23] D. Durban D and M. Baruch, "On the problem of a spherical cavity in an infinite elastoplastic medium," *J. Appl. Mech.,* vol. 43, pp. 633-638, 1976.
[24] V. K. Luk, M. J. Forrestal and D. E. Amos, "Dynamic spherical cavity expansion of strain-hardening materials," *J. Appl. Mech.,* vol. 58, pp. 1-6, 1991.
[25] Z. Rosenberg and E. Dekel, "Revisiting the perforation of ductile plates by sharp-nosed rigid projectiles," *Int. J. Solids Struct.,* vol. 47, pp. 3022-3033, 2010.
[26] Z. Rosenberg, R. Kositski and E. Dekel, "On the perforation of aluminium plates by 7.62 mm APM2 projectiles," *Int. J. Impact Eng.,* vol. 97, pp. 79-86, 2016.